

# Analytical description for the critical fixations of evolutionary coordination games on finite complex structured populations

Liye Zhang,<sup>1</sup> Yong Zou,<sup>1,2,\*</sup> Shuguang Guan,<sup>1,2</sup> and Zonghua Liu<sup>1,2</sup>

<sup>1</sup>*Department of Physics, East China Normal University, Shanghai 200062, China*

<sup>2</sup>*State Key Laboratory of Theoretical Physics, Institute of Theoretical Physics, Chinese Academy of Sciences, Beijing 100190, China*

(Received 25 December 2014; published 24 April 2015)

Evolutionary game theory is crucial to capturing the characteristic interaction patterns among selfish individuals. In a population of coordination games of two strategies, one of the central problems is to determine the fixation probability that the system reaches a state of networkwide of only one strategy, and the corresponding expectation times. The deterministic replicator equations predict the critical value of initial density of one strategy, which separates the two absorbing states of the system. However, numerical estimations of this separatrix show large deviations from the theory in finite populations. Here we provide a stochastic treatment of this dynamic process on complex networks of finite sizes as Markov processes, showing the evolutionary time explicitly. We describe analytically the effects of network structures on the intermediate fixations as observed in numerical simulations. Our theoretical predictions are validated by various simulations on both random and scale free networks. Therefore, our stochastic framework can be helpful in dealing with other networked game dynamics.

DOI: [10.1103/PhysRevE.91.042807](https://doi.org/10.1103/PhysRevE.91.042807)

PACS number(s): 89.75.Fb, 05.45.-a, 05.10.Gg, 87.23.Kg

## I. INTRODUCTION

Evolutionary game theory in general is an elegant way to understand the appearance of cooperation while abandoning the often problematic rationality assumption of the classical game theory [1,2]. Previously, evolutionary game dynamics has been mainly concentrated on regular structure, i.e., square lattices or well mixed populations [3], which hinges on the so-called “replicator equation” [2]. Deterministic replicator equations are helpful to understand the dynamics of infinite ( $N \rightarrow \infty$ ), homogeneous, and well mixed populations, describing the frequencies of the strategies in the population [2]. However, the insights provided by replicator dynamics may easily differ from the reality due to various reasons. For instance, the interaction patterns among human populations are rather heterogeneous in the sense that some people have more contacts with their friends than other people. It becomes even more challenging when facing populations of finite sizes so that one resorts largely to numerical simulations. Recently, much progress has been reported in the literature on game models on complex networks [4,5]. A large amount of effort has been devoted to uncovering the effects of heterogeneous population structures on individual’s strategy updating behaviors and hence on the macroscopic system’s dynamics [6,7]. Another helpful message provided by game models is to make fruitful suggestions on coping with free-riding incentives in public goods games as it is often discussed in the climate change mitigation processes [8].

Complex networks provide a natural and convenient framework to characterize the population structure, in particular with the heterogeneous interaction patterns in human society [5]. Given an unweighted, undirected network of  $N$  nodes, the degree  $k$  of node  $i$  is  $k_i = \sum_j A_{ij}$ , where  $A_{ij}$  are the elements of the symmetric adjacency matrix  $A$  ( $A_{ij} = 1$  when the nodes  $i$  and  $j$  are connected, and  $A_{ij} = 0$  if they are not connected).

On top of a complex network, various network dynamics can be implemented, ranging from synchronization [5,9] to epidemic spreading processes, etc. [10]. In a networked game model such as we consider, each link represents a game and the two nodes attached to this link are two players in the game. The number of games a player participated in varies over the population since each node of the network has potentially different degrees  $k$ . After one round, the payoff of player  $i$  accumulated from all games  $i$  is involved. A proper strategy updating rule is introduced before moving to the next step. There are many updating rules in the literature, most of which are based on imitation and learning [4,11,12]. One typical choice, for instance, is to compare the payoff of  $i$  to its peers. More specifically, we randomly choose a peer  $j \in \mathcal{N}_i$ , where  $\mathcal{N}_i$  is the neighborhood of  $i$ . Depending on the payoff difference, player  $i$  either sticks to its own strategy or switches to  $j$ ’s strategy in the next iteration. There are other networked game models in the literature, for instance, public goods games, which take place in the neighborhood  $\mathcal{N}_i$  [13].

In a population of two strategies, the replicator equation successfully discloses the most striking properties, that is fixation which refers to the probability for one strategy to take over the entire population, causing the extinction of the other strategy [14]. One more specific example is to assume that cooperation and defection are two strategies; the quantity of interest in this evolutionary process is the fixation probability of cooperators, i.e., the probability to end up in a state with  $N$  cooperators given that the initial number of cooperators is  $n$ . Another important quantity is the mean fixation time that the system needs to reach the final state. Evolutionary dynamics in finite-sized populations are not deterministic but stochastic. Stochastic processes represented by the Fokker-Plank equation can be used as computational tools in different areas, being useful descriptions of natural phenomena [15]. A stochastic framework was proposed to investigate the dynamic process of fixation in finite populations [14,16–18], providing more insight on the microscopic properties [19,20]. The difference between deterministic and stochastic modeling was further

\*Corresponding author: [yzou@phy.ecnu.edu.cn](mailto:yzou@phy.ecnu.edu.cn)

compared in [21–23]. The roles of noise and mutations on fixations have been demonstrated in [24–27]. Population structures and spatial constraints have certain influences on the strategy spreading dynamics [28–33] as well. Here, we show another message that the stochastic treatment yields a better description for the dynamic process of a finite-sized system.

In this work, we concentrate on coordination games on finite complex structured populations. For coordination games on well mixed populations of infinite size in particular, the system is bistable in the sense that the two boundary fixed points (all individuals have the same strategy, either of all type one or of all the other type) are absorbing [19]. The critical value of initial density of players of one strategy separating the two absorbing states corresponds to the unstable interior fixed point, above which the system evolves to 100% of one absorbing state. Therefore, this unstable fixed point yields an explosive jump of the fixation probability when passing this separatrix. However, the numerical estimation for this value is more challenging, which will be further explained by Fig. 1 in Sec. II. More specifically, there is a pronounced interval of an intermediate situation, that the system evolves to the absorbing state only with some probabilities. In other words, the system experiences a continuous transition from one absorbing state to the other. This intermediate fixation has been observed in populations of heterogeneous interaction topology, too. Here, we will analytically delineate the fixation probabilities and mean times given a finite population of complex structures, especially when the initial state is close to the unstable fixed point of discontinuity.

This paper is organized as follows. In Sec. II, we introduce the basics for the evolutionary coordination games on complex networks, and point out the importance of both population sizes and network structures on the numerical estimation of fixation probabilities. The general stochastic framework is proposed in Sec. III showing the fixation probability explicitly. Our results will be compared to the traditional replicator equations in Sec. IV. The conclusions are summarized in Sec. V.

## II. GAME MODEL AND CRITICAL FIXATION PROBABILITY

*Game model.* Assume that each link of the network represents a symmetric two-player game and the payoff matrix is expressed as

$$\mathcal{A} = \begin{pmatrix} & s_1 & s_2 \\ s_1 & a_{11} & a_{12} \\ s_2 & a_{21} & a_{22} \end{pmatrix}. \quad (1)$$

Each player has two strategies, either “ $s_1$ ” or “ $s_2$ .” Depending on the parameter settings in the payoff matrix  $\mathcal{A}$ , there are four generic cases [19] as follows. (i) Dominance. Either  $s_1$  dominates  $s_2$  ( $a_{11} > a_{21}$  and  $a_{12} > a_{22}$ ) or  $s_2$  dominates  $s_1$  ( $a_{11} < a_{21}$  and  $a_{12} < a_{22}$ ), for instance, Prisoner’s dilemma. (ii) Bistability ( $a_{11} > a_{21}, a_{22} > a_{12}$ ). (iii) Coexistence ( $a_{11} < a_{21}$  and  $a_{12} > a_{22}$ ). (iv) Neutrality ( $a_{11} = a_{21}$  and  $a_{12} = a_{22}$ ). In this work, we impose the condition (ii) such that we have coordination games.

*Strategy updating rules.* We concentrate on pairwise payoff comparison processes [19]. In particular, time is divided into discrete periods. At the end of each period, player  $i$  decides whether to keep its current action or to adopt the action of one of its neighboring player  $j$ , depending on the current payoff difference between  $i$  and  $j$ ,  $u_i - u_j$ . The payoff  $u_i$  is accumulated in the neighborhood of  $i$  as  $u_i = \sum_{l=1}^N A_{il} s_l \mathcal{A} s_l$ , where  $\mathcal{A}$  is the payoff matrix. Note that  $u_i$  does not include  $i$ ’s history into account. Then, the player  $i$  randomly selects one neighbor  $j$  from its neighborhood  $\mathcal{N}_i$  and switches to  $j$ ’s action in the next round with a probability

$$w_{s_i \rightarrow s_j} = \frac{1}{1 + \exp^{(u_i - u_j)/\kappa}}, \quad (2)$$

where  $\kappa$  denotes the noise amplitude characterizing the level of rationality of individuals, which is often chosen as  $\kappa = 0.1$  following the previous works [34–36]. A smaller  $\kappa$  corresponds to a stronger influence of  $j$  on  $i$ . The larger the payoff difference between  $i$  and  $j$ , the higher probability  $i$  tends to adopt  $j$ ’s action in the next round.

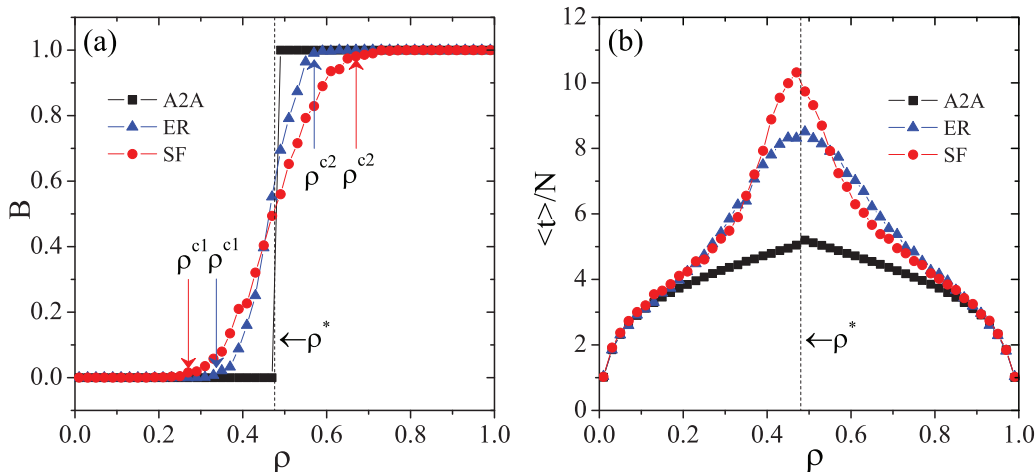


FIG. 1. (Color online) (a) Fixation probabilities  $B$  to pure  $s_1$  players, and (b) mean fixation times  $\langle t \rangle / N$ . Network size  $N = 100$ , and mean degree  $\langle k \rangle = 6$ . Payoff matrix is  $a_{11} = 1.2, a_{12} = 0, a_{21} = 0.1, a_{22} = 1$  and  $\kappa = 0.1$ . The unstable fixed point  $\rho^*$  is highlighted. Erdos-Renyi random networks ( $\blacktriangle$ ), scale free networks ( $\bullet$ ), and all-to-all connected (well mixed) population ( $\blacksquare$ ).

*Critical fixation probability.* In a well mixed population where each individual is equally likely to interact with any other individual, the mean-field description by continuous replicator dynamics has led to much insight [16]. In the particular coordination game with two strategies, the quantity of interest is to study the density of individuals adopting the strategy of  $s_1$  which is denoted by  $\rho_{s_1}$ . There are three equilibrium points: two absorbing boundary points  $\rho_{s_1} = 0$  and  $\rho_{s_1} = 1$ , and one unstable interior fixed point  $\rho^*$  which reads

$$\rho^* = \frac{a_{22} - a_{12}}{a_{11} + a_{22} - a_{12} - a_{21}}. \quad (3)$$

The resulted replicator equation of the system exhibits bistability, which shows discontinuity at  $\rho^*$  separating the absorbing state  $\rho_{s_1} = 0$  from  $\rho_{s_1} = 1$ . For a critical value of frequencies above  $\rho^*$ , the population evolves toward 100% of pure  $s_1$  individuals [16,22]. Given an initial density  $\rho_{s_1}$  at time  $t$ , the system eventually will be absorbed at any of the two boundary states with probability 1.

We denote the fixation probability as  $B$  that the system reaches the absorbing boundary at  $\rho_{s_1} = 1$ , and the corresponding asymptotic expectation times as  $\langle t \rangle$ . Both  $B$  and  $\langle t \rangle$  are important quantities to characterize the evolutionary process. Typically, simulations on finite populations with complex structures show large deviations from the replicator's prediction, namely a pronounced interval ( $\rho^{c1}, \rho^{c2}$ ) around  $\rho^*$  has been observed as shown in Fig. 1. In other words, the simulations of Fig. 1 show convincingly a continuous monotonic increasing, while the replicator equation predicts an abrupt jump at  $\rho^*$ . This interval suggests an intermediate regime that the probability for the system to reach the state of all  $s_1$  individuals is less than 1. There are two crucial ingredients in this discrepancy: finite size  $N$  of the populations and the underlying network structures.

Therefore, numerical estimation of the critical fixation probability remains ambiguous, in particular when the initial density  $\rho_{s_1}$  of  $s_1$  individuals is close to the unstable fixed point  $\rho^*$ . Furthermore, we find that the variance around  $\rho^*$  becomes larger in scale free networks. In this work, we delineate the interval for  $\Delta\rho = (\rho^{c2} - \rho^{c1})$  analytically by a stochastic modeling approach, while taking into consideration the network structures.

### III. STATE TRANSITION MATRIX AND MEAN FIXATION TIMES

We consider coordination games on top of a complex network which is characterized by the degree distribution  $P(k)$ . In a population of  $N$  players, we first use the mean-field method to obtain some theoretical understandings. Later we consider the case of  $N \rightarrow \infty$ , retrieving the traditional replicator equations from the stochastic process.

Without loss of generality, we suppose that at time  $t$  the probability to have  $n$  nodes out of  $N$  players having  $s_1$  strategy is  $\phi_n = f(n, t)$ . There are  $N + 1$  possible states  $\phi_0, \phi_1, \dots, \phi_n, \dots, \phi_N$ . The network state at time  $t$  is hence represented by a vector  $f(\mathbf{n}, t) = (f(0, t), f(1, t), \dots, f(n, t), \dots, f(N, t))$ , which fulfills the normalization  $\sum_{n=0}^N f(n, t) = 1$ . There are two absorbing

states: (i)  $f(0, t)$  corresponds to the case of zero players having strategy  $s_1$  (or all are  $s_2$  players), and (ii)  $f(N, t)$  means that the whole network is full of  $s_1$  strategy. The network state at time  $t + 1$  is represented by

$$f(\mathbf{n}, t + 1) = f(\mathbf{n}, t)M, \quad (4)$$

where  $M$  is the network state transition matrix. In the next step, we study the dynamics based on  $M$ .

The mean-field approximation assumes that, in the neighborhood of node  $i$ , there is a fraction of  $n/N$  players in state  $s_1$ , namely, at time  $t$ ,

$$\rho_{s_1}(j, t) = \frac{n}{N}, \quad \forall j \in \mathcal{N}_i, \quad (5)$$

where  $\mathcal{N}_i$  is the neighborhood of node  $i$ . We note that there are no differences in the results below if one replaces the subscript  $s_1$  by  $s_2$ , therefore, we omit it in the following. In the next round  $t + 1$ , the transition probability that the number of  $s_1$  players is increased to  $n + 1$  can be expressed as

$$T_+(n) = \sum_{k=0}^{\infty} P(k)(1 - \rho) \sum_{k'=0}^{\infty} P(k'|k)\rho w(u_k^+, u_{k'}^+), \quad (6)$$

$$= (1 - \rho)\rho \sum_{k=0}^{\infty} P(k) \sum_{k'=0}^{\infty} P(k'|k)w(u_k^+, u_{k'}^+), \quad (7)$$

where  $k$  is the degree of node  $i$ ;  $P(k)$  is the probability to have a node of degree  $k$ ;  $P(k'|k)$  is the conditional probability that a link from a node of degree  $k$  points to a node of degree  $k'$ ;  $u_k^+$  is the payoff of degree  $k$  when taking action of  $s_2$  and  $u_{k'}^+$  is the payoff of degree  $k'$  when having action of  $s_1$ , while  $w(u_k^+, u_{k'}^+)$  is the probability to switch to  $s_1$  in the next round. More specifically,

$$w(u_k^+, u_{k'}^+) = 1/\{1 + \exp[(u_k^+ - u_{k'}^+)/\kappa]\}, \quad (8)$$

$$u_k^+ = k[\rho a_{21} + (1 - \rho)a_{22}], \quad u_{k'}^+ = k'[\rho a_{11} + (1 - \rho)a_{12}]. \quad (9)$$

When obtaining Eqs. (6) and (7), we assume that the strategy updating of player  $i$  is independent of its degree  $k$ . The mean-field approximation further requires that the variance of the degree sequence  $k_i$  is small, for instance, the mean degree of a network  $\langle k \rangle$  should not be too small. However, our numerical simulations below show that sparser networks of small values of  $\langle k \rangle$  yield good agreements to the theoretical predictions as well.

In a full analogy, in the next iteration  $t + 1$ , the transition probability that the number of  $s_1$  players is decreased to  $n - 1$  reads

$$T_-(n) = \rho(1 - \rho) \sum_{k=0}^{\infty} P(k) \sum_{k'=0}^{\infty} P(k'|k)w(u_k^-, u_{k'}^-), \quad (10)$$

where  $w(u_k^-, u_{k'}^-)$  is the probability to switch to  $s_2$  in the next round, in particular,

$$w(u_k^-, u_{k'}^-) = 1/\{1 + \exp[(u_k^- - u_{k'}^-)/\kappa]\}, \quad (11)$$

$$u_k^- = k[\rho a_{11} + (1 - \rho)a_{12}], \quad u_{k'}^- = k'[\rho a_{21} + (1 - \rho)a_{22}]. \quad (12)$$

The probability to keep  $n$   $s_1$  players unchanged at time  $t + 1$  is given by

$$T_0(n) = 1 - T_+(n) - T_-(n). \quad (13)$$

We note that  $T_+(0) = T_-(N) = 0$  since the two boundary states are absorbing. Additionally,  $\Delta T(n) = T_+(n) - T_-(n)$ .

Therefore, the state transition matrix of the network is obtained as

$$M = \begin{pmatrix} 1 & 0 & 0 & 0 & \cdots & 0 \\ T_-(1) & T_0(1) & T_+(1) & 0 & & 0 \\ 0 & T_-(2) & T_0(2) & T_+(2) & & 0 \\ \vdots & & & & \ddots & \vdots \\ 0 & 0 & 0 & 0 & \cdots & 1 \end{pmatrix} = \begin{pmatrix} I_2 & 0 \\ R & Q \end{pmatrix}, \quad (14)$$

where

$$I_2 = \begin{pmatrix} 1 & 0 \\ 0 & 1 \end{pmatrix}, \quad R = \begin{pmatrix} T_-(1) & 0 \\ 0 & 0 \\ \vdots & \vdots \\ 0 & T_+(N-1) \end{pmatrix}, \quad Q = \begin{pmatrix} T_0(1) & T_+(1) & 0 & \cdots \\ T_-(2) & T_0(2) & T_+(2) & \\ \vdots & & & \ddots \\ 0 & 0 & 0 & \cdots & T_0(N-1) \end{pmatrix}, \quad (15)$$

and  $I_2$  represents the two absorbing states,  $R$  is for the system to reach the absorbing states in one step, and  $Q$  is the transition probabilities for any transient states. We further denote the following two matrices:

$$H = (I_{N-1} - Q)^{-1} \quad (16)$$

$$= \begin{pmatrix} T_+(1) + T_-(1) & -T_+(1) & 0 & \cdots \\ -T_-(2) & T_+(2) + T_-(2) & -T_+(2) & \\ \vdots & & & \ddots \\ 0 & 0 & 0 & \cdots & T_+(N-1) + T_-(N-1) \end{pmatrix}^{-1}, \quad (17)$$

$$B = HR = \begin{pmatrix} H_{11}T_-(1) & H_{1(N-1)}T_+(N-1) \\ H_{21}T_-(1) & H_{2(N-1)}T_+(N-1) \\ \vdots & \vdots \\ H_{(N-1)1}T_-(1) & H_{(N-1)(N-1)}T_+(N-1) \end{pmatrix}. \quad (18)$$

Note that the matrix  $I_{N-1} - Q$  is tridiagonal, the inverse of which determines the stochastic dynamics of the system, namely, the fixation probabilities and the average times that are necessary for the system to reach the absorbing states (note that a brief introduction to the matrix  $H$  is provided in the Appendix and more details can be found in [15]). More specifically, starting from any initial state  $S_I(0)$ ,  $I \in [1, N-1]$ , we have the probabilities  $B_{I2}$  and  $B_{I1}$  that the system is attracted to the absorbing state of all  $s_1$  players, respectively, of all  $s_2$  players. Furthermore, the mean fixation time that the system is attracted to the absorbing state from any initial state  $I$  reads

$$\langle t_I \rangle = \sum_{m=1}^{N-1} H_{Im}. \quad (19)$$

For the purpose of comparison between networks of different sizes, one normalizes it by the number of nodes in the network, namely,  $\langle t_I \rangle / N$ . Some recipes for estimating the inverse of a general tridiagonal matrix are presented in [37].

### A. Numerical results

The numerical simulations are presented in this section, which agree with the theories above. We note that we run simulations on 100 random networks, each of which has 1000 realizations. In total, each dot in all figures through-

out the paper is an average over  $10^5$  random realizations. More specifically, we run simulations on both Erdos-Renyi random and scale free networks to check the two transition probabilities  $T_+(n)$  and  $T_-(n)$  [Figs. 2(a) and 2(e)],  $\Delta T(n)$  [Figs. 2(b) and 2(f)], fixation probabilities  $B$  [Figs. 2(c) and 2(g)], and the corresponding expectation time  $\langle t \rangle / N$  [Figs. 2(d) and 2(h)]. Note that the numerical estimations for the fixation probabilities  $B$  show monotonic increasing trends, instead of abrupt jumps, when  $\rho$  is close to  $\rho^*$ . These results have been validated by a different choice of the payoff matrix as shown in Fig. 3. The increase of  $a_{21}$  from 0.1 to 0.8 changes the position of  $\rho^*$ , which indicates that the system asymmetrically favors one stable equilibrium over the other.

### B. Deterministic equation of the expectation density

Next, we obtain the replicator equation when  $N \rightarrow \infty$ . Let us start by considering the dynamics of the expectation value of the density of  $s_1$  players at time  $t$ , which we denote as  $\bar{\rho}$ . Based on the state transition matrix  $M$  [Eq. (14)], we expand the network state at time  $t + 1$  [Eq. (4)] as

$$\begin{aligned} f(n, t+1) &= T_+(n-1)f(n-1, t) + T_0f(n, t) \\ &\quad + T_-(n+1)f(n+1, t), \quad 1 \leq n \leq N-1. \end{aligned} \quad (20)$$

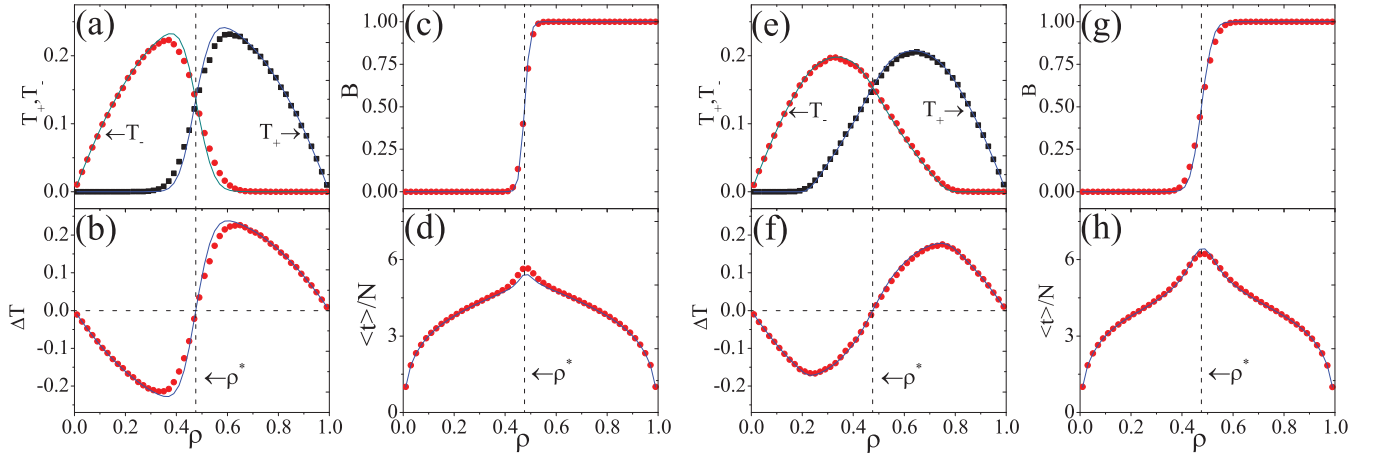


FIG. 2. (Color online) Simulations on complex networks ( $N = 100$  and mean degree  $\langle k \rangle = 20$ ). Payoff matrix is  $a_{11} = 1.2, a_{12} = 0, a_{21} = 0.1, a_{22} = 1$  and  $\kappa = 0.1$ . Dots are numerical simulations, while solid lines are from the theory. The unstable fixed point  $\rho^*$  is denoted by the vertical dashed line. (a)–(d) Erdos-Renyi random networks; (e)–(h) scale free networks generated by Barabási-Albert algorithm. (a), (e)  $T_+(n)$  (■), Eq. (7) and  $T_-(n)$  (●), Eq. (10); (b), (f)  $\Delta T$ ; (c), (g) fixation probabilities  $B$  to pure  $s_1$  strategy; (d), (h) mean fixation times  $\langle t \rangle / N$ .

The two absorbing states corresponding to  $n = 0$  and  $n = N$  are respectively represented by

$$f(0, t + 1) = T_0(0)f(0, t) + T_-(1)f(1, t), \quad (21)$$

$$f(N, t + 1) = T_+(N - 1)f(N - 1, t) + T_0(N)f(N, t). \quad (22)$$

Since Eq. (13), the stochastic dynamics of the network is described by the master equation as

$$\frac{\Delta f(n, t)}{\Delta t} = f(n, t + 1) - f(n, t) \quad (23)$$

$$= T_+(n - 1)f(n - 1, t) - [T_+(n) + T_-(n)]f(n, t) + T_-(n + 1)f(n + 1, t). \quad (24)$$

Again, the two absorbing states of  $n = 0$  and  $n = N$  are the following:

$$\frac{\Delta f(0, t)}{\Delta t} = T_-(1)f(1, t), \quad (25)$$

$$\frac{\Delta f(N, t)}{\Delta t} = T_+(N - 1)f(N - 1, t). \quad (26)$$

Therefore, the expectation of the density of  $s_1$  players in the network is

$$\bar{\rho} = \frac{1}{N} \sum_{n=0}^N n f(n, t), \quad (27)$$

which leads to the variation of the probability density per unit time as

$$\frac{\Delta \bar{\rho}}{\Delta t} = \frac{1}{N} \sum_{n=0}^N n \frac{\Delta f(n, t)}{\Delta t}. \quad (28)$$

Putting the conditions [Eqs. (23), (25), and (26)] into Eq. (28), we have

$$\begin{aligned} \frac{\Delta \bar{\rho}}{\Delta t} = & \frac{1}{N} \sum_{n=1}^{N-1} n \times \{T_+(n - 1)f(n - 1, t) \\ & - [T_+(n) + T_-(n)]f(n, t) + T_-(n + 1)f(n + 1, t)\} \\ & + 0 \times T_-(1)f(1, t) + N \times T_+(N - 1)f(N - 1, t), \end{aligned}$$

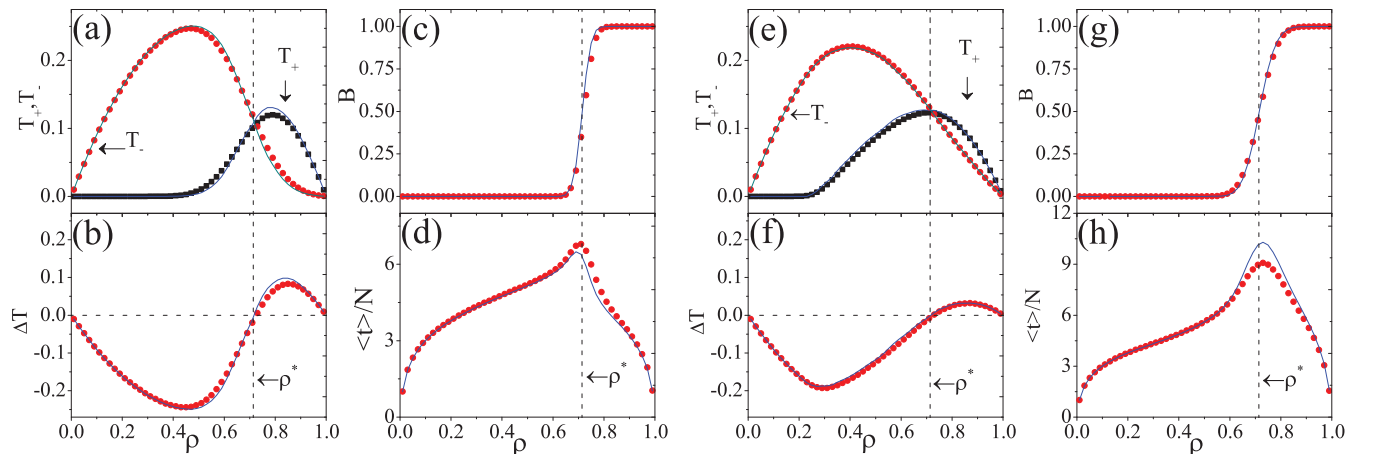


FIG. 3. (Color online) Caption is the same as in Fig. 2, except  $a_{21}$  is equal to 0.8 in the payoff matrix.

$$= \frac{1}{N} \sum_{n=1}^{N-1} [T_+(n) - T_-(n)] f(n, t), \quad (29)$$

where  $f(n, t)$  fulfills the normalization  $\sum_{n=0}^N f(n, t) = 1$ . Equation (29) is the variation of the expectation of the density of strategy  $s_1$  in the population given the distribution  $f(n, t)$  at time  $t$ . Due to the diffusive property of the process,  $f(n, t)$  is a  $\delta$ -like function centered at the mean value  $\bar{n}$ , in particular with the following approximation:

$$f(n, t) = \begin{cases} f(n, t) = 1, & n = \bar{n}, \\ f(n, t) = 0, & n \neq \bar{n}. \end{cases} \quad (30)$$

Based on Eq. (29), a continuous process is obtained in the limit ( $\Delta t \rightarrow 0, N \rightarrow \infty$ ), with a dimensionless time  $\tau = t/N$ ,

$$\frac{d\bar{\rho}}{d\tau} = T_+(\bar{\rho}) - T_-(\bar{\rho}). \quad (31)$$

Taking conditions [Eqs. (7) and (10)] into account, the right-hand side of Eq. (31) is a nonlinear function of  $\bar{\rho}$  as follows:

$$T_+(\bar{\rho}) - T_-(\bar{\rho}) = \bar{\rho}(1 - \bar{\rho}) \sum_{k=0}^{\infty} P(k) \sum_{k'=0}^{\infty} P(k'|k) [w(u_k^+, u_{k'}^+) - w(u_k^-, u_{k'}^-)]. \quad (32)$$

The fixed points of the above deterministic equation (31) are determined by  $T_+(\bar{\rho}) - T_-(\bar{\rho}) = 0$ , i.e., the transition probabilities of both birth-death rates are balanced. Furthermore, it is easy to show there are three fixed points: two absorbing fixed points  $\bar{\rho} = 0$  (pure  $s_2$ ),  $\bar{\rho} = 1$  (pure  $s_1$ ), and one unstable fixed point  $\bar{\rho} = \rho^*$  noting  $\bar{\rho}a_{21} + (1 - \bar{\rho})a_{22} = \bar{\rho}a_{11} + (1 - \bar{\rho})a_{12}$ , and  $w(u_k^+, u_{k'}^+) = w(u_k^-, u_{k'}^-)$  at  $\bar{\rho} = \rho^*$ . Therefore, the results by replicator equations are fully recovered.

### C. Comparisons to well-mixed populations

Next, we show that the case of well mixing (for a finite  $N$ ) can be regarded as a special case of the above theory. Suppose at time  $t$  there are  $n$  players out of the population size  $N$  taking  $s_1$  strategy. Thus the probability to choose an  $s_1$  player is  $n/N$  and, respectively, an  $s_2$  player from the remaining population is  $(N - n)/(N - 1)$ . The payoffs  $u_{s_1}$  of the  $s_1$  player, respectively,  $u_{s_2}$  of the  $s_2$  player read

$$u_{s_1} = (N - 1)[\rho a_{21} + (1 - \rho)a_{22}], \quad (33)$$

$$u_{s_2} = (N - 1)[\rho a_{11} + (1 - \rho)a_{12}]. \quad (34)$$

The transition probability  $T_+(n)$  is expressed as

$$T_+(n) = \frac{n(N - n)}{N(N - 1)} w_{s_2 \rightarrow s_1} \approx \rho(1 - \rho) w_{s_2 \rightarrow s_1}, \quad (35)$$

where  $w_{s_2 \rightarrow s_1} = 1/[1 + \exp^{(u_{s_2} - u_{s_1})/\kappa}]$  is the special case of the strategy updating rule [Eq. (2)]. Similarly,  $T_-(n)$  reads

$$T_-(n) \approx \rho(1 - \rho) w_{s_1 \rightarrow s_2}, \quad (36)$$

where  $w_{s_1 \rightarrow s_2}$  is again the special case of Eq. (2). Therefore,  $\Delta T$  is simplified as

$$\Delta T(n) = T_+(n) - T_-(n) = \rho(1 - \rho)(w_{s_2 \rightarrow s_1} - w_{s_1 \rightarrow s_2}). \quad (37)$$

It is reasonable to use the Heaviside function to replace the strategy updating rule since a small  $\kappa$  is often used, namely,

$$(w_{s_2 \rightarrow s_1} - w_{s_1 \rightarrow s_2}) = \begin{cases} 1, & \rho = \frac{n}{N} \geq \rho^*, \\ -1, & \rho = \frac{n}{N} < \rho^*. \end{cases} \quad (38)$$

Therefore, the system shows an explosive jump at  $\rho^*$  when the population evolves toward 100% of pure  $s_1$  individuals.

Equations (35) and (36) can be directly derived from Eqs. (7) and (10) by taking into account the following conditions:

$$P(k) = \begin{cases} 1, & k = N - 1, \\ 0, & \text{else,} \end{cases} \quad (39)$$

$$P(k'|k) = \begin{cases} 1, & k = k' = N - 1, \\ 0, & \text{else.} \end{cases}$$

Figure 4 illustrates the numerical results, showing an excellent agreement to the above theory. In contrast, when considering network structures, the system shows a continuous transition at  $\rho^*$  as compared in Fig. 4.

## IV. VARIANCE OF NUMERICALLY ESTIMATED $\rho^c$

The replicator dynamics is a useful framework to explore the general dynamics of an unstructured population when  $N \rightarrow \infty$ . So far, we have shown convincingly that an explosive jump is absent for a finite system switching from one absorbing state to the other. Around the unstable fixed point  $\rho^*$ , we show explicitly that there is a substantial interval  $(\rho^{c1}, \rho^{c2})$  which explains the continuous transitions as observed in numerical simulations. For populations of finite sizes, the evolutionary dynamics is stochastic, which prompts one to use a Fokker-Plank equation for the description. The crucial step is to determine the regime where the diffusion term plays a significant role in deciding the macroscopic behavior.

To that end, we introduce the notations  $\rho = n/N$ ,  $\tau = t/N$  in the master equation [Eq. (24)]. Based on the theory in [19,21], for  $N \gg 1$  the probability densities and transition probabilities are expanded in a Taylor series at  $\rho$  and  $\tau$ , which yield the following Fokker-Plank equation (details are in [19]):

$$\frac{\partial}{\partial \tau} f(\rho, \tau) = -\frac{\partial}{\partial \rho} [a(\rho) f(\rho, \tau)] + \frac{1}{2} \frac{\partial^2}{\partial \rho^2} [b^2(\rho) f(\rho, \tau)] + O(N^{-2}), \quad (40)$$

where

$$a(\rho) = T_+(\rho) - T_-(\rho), \quad b(\rho) = \sqrt{\frac{1}{N} [T_+(\rho) + T_-(\rho)]}, \quad (41)$$

and  $a(\rho)$  is the drift and  $b(\rho)$  is the diffusion coefficient. We consider the relative contributions between the drift and diffusion terms by

$$\left| \frac{b^2(\rho^c)}{a(\rho^c)} \right| = \frac{(1/N)[T_+(\rho^c) + T_-(\rho^c)]}{|T_+(\rho^c) - T_-(\rho^c)|} = \eta, \quad (42)$$

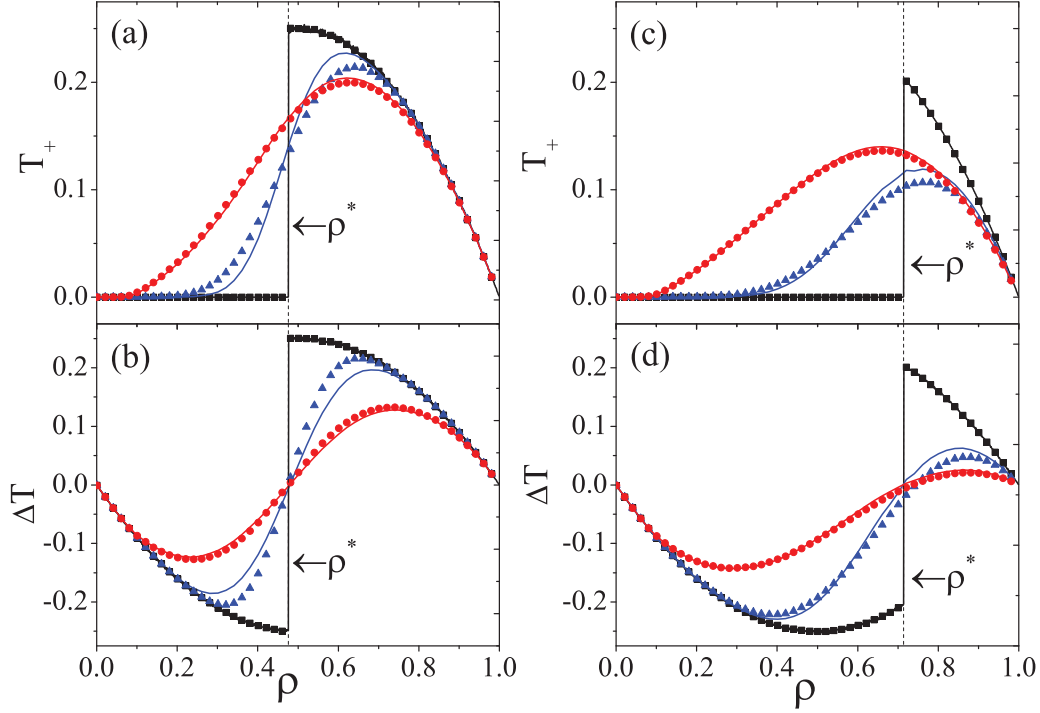


FIG. 4. (Color online) Comparisons to the well mixed population. (a), (c)  $T_+(n)$  [Eq. (35)]; (b), (d)  $\Delta T(n)$  [Eq. (37)]. Payoff matrix is  $a_{11} = 1.2, a_{12} = 0, a_{22} = 1$  (a), (b)  $a_{21} = 0.1$  (c), (d)  $a_{21} = 0.8$ . ER random networks ( $\blacktriangle$ ), scale free networks ( $\bullet$ ), and well-mixed (all-to-all connected) networks ( $\blacksquare$ ). Solid lines are the corresponding theoretical predictions.

where  $\rho^c$  is the critical density value when the diffusion reaches a given level  $\eta$  relevant to the drift term.<sup>1</sup> There is another way to study the role of the diffusion term [38].

Equation (40) is reduced to the deterministic replicator dynamics [Eq. (31)] when  $N \rightarrow \infty$  since the diffusion term

$b(\rho)$  vanishes with  $1/\sqrt{N}$  and  $\eta \approx 0$ . In contrast, for a finite value of  $N$ , the diffusion term has to be considered as significant when the system is close to the interior fixed point  $\rho^*$  since  $T_+(\rho^c) - T_-(\rho^c) \approx 0$ . Substituting Eqs. (6) and (10) into Eq. (42), we have

$$\frac{|\sum_{k=0}^{\infty} P(k) \sum_{k'=0}^{\infty} P(k'|k) w(u_k^+, u_{k'}^+) - \sum_{k=0}^{\infty} P(k) \sum_{k'=0}^{\infty} P(k'|k) w(u_k^-, u_{k'}^-)|}{\sum_{k=0}^{\infty} P(k) \sum_{k'=0}^{\infty} P(k'|k) w(u_k^+, u_{k'}^+) + \sum_{k=0}^{\infty} P(k) \sum_{k'=0}^{\infty} P(k'|k) w(u_k^-, u_{k'}^-)} = \frac{1}{N\eta}. \quad (43)$$

When a small value of  $\kappa$  is used, we use the Heaviside function to replace the rules for strategy updating [Eqs. (8) and (11)], namely,

$$w(u_k^+, u_{k'}^+) \approx H(u_{k'} - u_k) = \begin{cases} 1, & u_{k'} \geq u_k, \\ 0, & u_{k'} < u_k, \end{cases} \quad (44)$$

$$w(u_k^-, u_{k'}^-) \approx H(u_{k'}' - u_k') = \begin{cases} 1, & u_{k'}^- \geq u_k^-, \\ 0, & u_{k'}^- < u_k^-. \end{cases} \quad (45)$$

Given the above two conditions [Eqs. (44) and (45)], Eq. (43) can be further simplified

as

$$\frac{\sum_{k=0}^{\infty} P(k) \sum_{k'=\min\{\gamma k, \frac{1}{\gamma} k\}}^{\max\{\gamma k, \frac{1}{\gamma} k\}} P(k'|k)}{\sum_{k=0}^{\infty} P(k) [\sum_{k'=\gamma k}^{\infty} P(k'|k) + \sum_{k'=\frac{1}{\gamma} k}^{\infty} P(k'|k)]} = \frac{1}{N\eta}, \quad (46)$$

where

$$\gamma = \frac{\rho^c a_{21} + (1 - \rho^c) a_{22}}{\rho^c a_{11} + (1 - \rho^c) a_{12}}, \quad 0 \leq \rho^c \leq 1. \quad (47)$$

Note that  $\gamma$  shows the relationship between the network structure  $P(k)$  [Eq. (46)] and the payoffs [Eq. (47)]. Furthermore, we show that both  $\gamma$  and  $\frac{1}{\gamma}$  are solutions to Eq. (46). A schematic illustration to understand Eq. (46) is shown in Fig. 5. The drift term is proportional to the numerator and, respectively, the diffusion is proportional to the denominator of Eq. (46). More specifically,  $a(\rho) \propto S_2$  and  $b^2(\rho) \propto (S_2 + 2S_1)$ . It is easy to show that the unstable interior

<sup>1</sup>In numerical simulations,  $\eta$  can be adaptively chosen according to the probability that the system deviates from full  $s_2$  or full  $s_1$  strategy by some suitable level, for instance, 1% deviation from the two absorbing states.

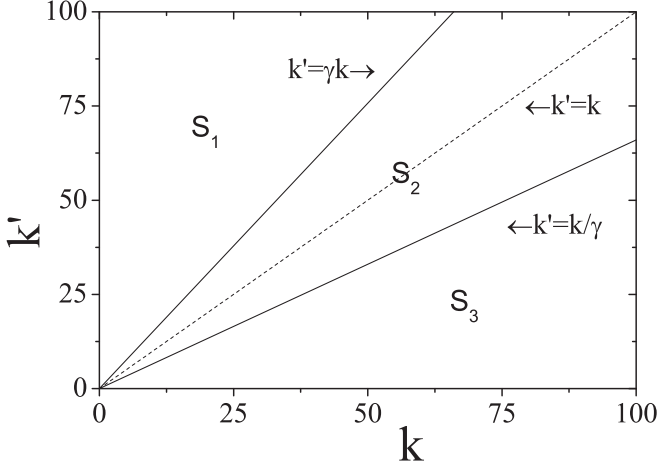


FIG. 5. Schematic illustration for Eq. (46), the numerator of which is shown by the area  $S_2$ .

fixed point  $\rho^*$  yields  $\gamma = 1$ , corresponding to the case that the drift term  $a(\rho)$  is degenerated to be zero, as shown by the area  $S_2$  tends to zero in Fig. 5.

One can prove that the denominator of Eq. (46) becomes 1 provided  $P(k'|k) = P(k')$  when one assumes no degree-degree correlations are present in a network. In particular, Eq. (46) is simplified as

$$\sum_{k=0}^{\infty} P(k) \sum_{k'=\min\{\gamma k, \frac{1}{\gamma}k\}}^{\max\{\gamma k, \frac{1}{\gamma}k\}} P(k') = \frac{1}{N\eta}. \quad (48)$$

Given the degree distribution  $P(k)$  and conditional degree distribution  $P(k'|k)$  of a network, one calculates  $\gamma$  from Eq. (46). Then, one computes the critical density of  $\rho^c$  as follows:

$$\rho^{c1} = \frac{a_{22} - \gamma a_{12}}{\gamma a_{11} + a_{22} - \gamma a_{12} - a_{21}}, \quad (49)$$

$$\rho^{c2} = \frac{a_{22} - \frac{1}{\gamma} a_{12}}{\frac{1}{\gamma} a_{11} + a_{22} - \frac{1}{\gamma} a_{12} - a_{21}}. \quad (50)$$

Without loss of generality, we assume that  $0 < \rho^{c1} \leq \rho^{c2} < 1$ . Therefore, the difference  $\Delta\rho = \rho^{c2} - \rho^{c1}$  defines the deviation of the numerical estimation of  $\rho^c$  from the predicted value  $\rho^*$ .

Both Eqs. (46) and (48) describe precisely the roles of network structures on the critical values of fixation probability when  $\rho$  is close to  $\rho^*$ . Depending on the initial density  $\rho$  of  $s_1$ , we have the following situations.

(1) The deterministic replicator equation successfully captures the dynamics when  $\rho \in (0, \rho^{c1}) \cup (\rho^{c2}, 1)$ . In contrast, when  $\rho \in (\rho^{c1}, \rho^{c2})$ , the diffusion term becomes essential such that  $b^2(\rho) > \eta|a(\rho)|$  and, therefore, the approximation by replicator equation becomes imprecise.

(2) The unstable interior fixed point  $\rho^*$  is in the interval of  $\rho^* \in (\rho^{c1}, \rho^{c2})$ , which corresponds to the case that the drift term  $a(\rho)$  is degenerated to be zero. Therefore, when  $\rho \approx \rho^*$ , we have  $b^2(\rho) \gg |a(\rho)|$ , namely, replicator dynamics shows large fluctuations around  $\rho^*$ .

(3) For networks of high link densities, one has rather large mean degree  $\langle k \rangle$ . In this case, we have  $\rho^{c1} \approx \rho^{c2}$  provided there is no pronounced difference between  $\min\{\gamma k, \frac{1}{\gamma}k\}$  and  $\max\{\gamma k, \frac{1}{\gamma}k\}$  [Eq. (46)]. This often appears in all-to-all connected or well-mixed networks, where the interval  $\Delta\rho$  around  $\rho^*$  is neglectable, which agrees with our approximations discussed in Sec. III C.

(4) For sparser networks like scale free or ER random networks of low mean degrees  $\langle k \rangle$ , the interval of  $\Delta\rho$  becomes substantive and one observes the large deviation of the numerical estimation of  $\rho^c$  from the prediction  $\rho^*$ . Furthermore, it is expected that  $\Delta\rho$  is larger for scale free networks than that for ER random networks. In conclusion, it is the heterogeneous property in the degree distribution that leads to the significant difference between  $\rho^{c1}$  and  $\rho^{c2}$ .

The above statements have been consistently validated by the numerical estimation of fixation probability  $B$  and the corresponding expectation times, as shown in Fig. 1. Furthermore, as the mean degree  $\langle k \rangle$  of a network is increased, one moves from a situation of heterogeneous interaction topology to the situation as fulfilled by well mixing populations. Therefore, the interval of  $\Delta\rho$  decreases when one increases  $\langle k \rangle$  (shown in Fig. 6), converging to the results as predicted by replicator equations for all-to-all connection. Note that  $\Delta\rho$  is larger in scale free networks than that of ER random networks when  $\langle k \rangle$  is systematically increased.

*Effects of selection strength.* Concerning the noise level of irrationality  $\kappa$ , we followed the traditional way to choose  $\kappa = 0.1$  in the stochastic strategy updating rule [Eq. (2)] [34,35,39–41]. Our results do not change qualitatively if  $\kappa$  is varied in a suitable interval, for instance,  $\kappa \in (0.0001, 1.0)$ , as shown in Fig. 7. The nonvanishing interval  $\Delta\rho$  has been obtained for rather small values of  $\kappa$  (order of  $10^{-4}$ ). In contrast, for well-mixed populations (e.g., all-to-all connected), we find that  $\Delta\rho \approx 0$ . Therefore, we conclude that the gradual monotonic increasing trends of the fixation probabilities at  $\rho^*$  are genuine properties of the processes.

A smaller  $\kappa$  corresponds to a relative strong selection for strategy spreading. An interesting limiting case is to consider  $\kappa \rightarrow 0$  [42], which yields a fully deterministic process for arbitrary population size. The strategy updating rule [Eq. (2)] is reduced to unconditional imitations depending only on the sign of the payoff difference. In contrast, a large value of  $\kappa$  suggests that the approximation by Eqs. (44) and (45) becomes imprecise, since this indicates a weak selection strength in the strategy updating. It is expected that the interval  $(\rho^{c1}, \rho^{c2})$  becomes wider for much larger  $\kappa$ . The limit of  $\kappa \rightarrow \infty$  is reduced to the case of neutral selection; the fixation probabilities are a linear function of  $\rho$  [19]. In consequence,  $\Delta\rho \rightarrow 1$  when  $\kappa$  is larger than 100 as shown in Fig. 7.

## V. CONCLUSIONS

The numerical estimation for the intermediate fixation probabilities for populations of finite sizes shows large deviations from the unstable interior fixed point  $\rho^*$  which was predicted by the replicator equations. We propose a stochastic framework to study the evolutionary process of the networked coordination games, which explains clearly the numerical

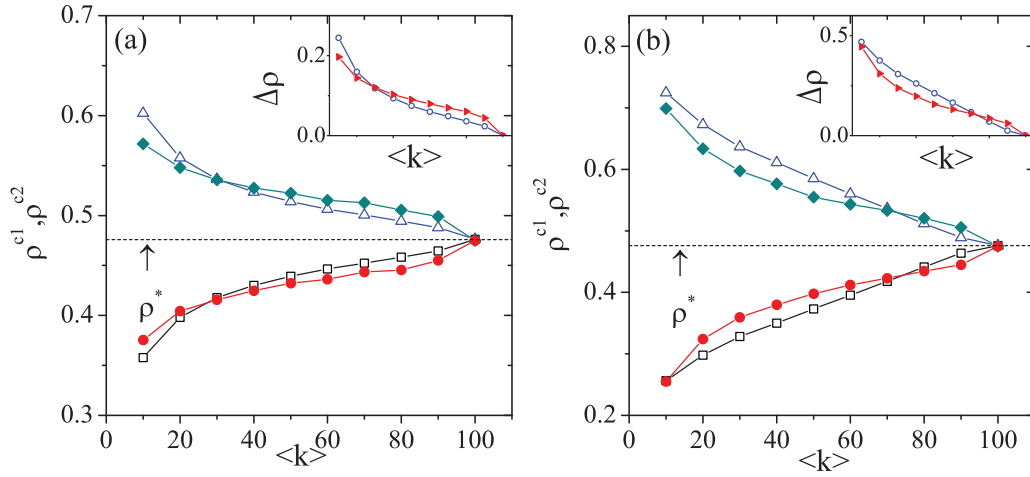


FIG. 6. (Color online)  $\rho^{c1}$  and  $\rho^{c2}$  vs  $\langle k \rangle$ , while insets are  $\Delta\rho$  for the corresponding networks. Open squares  $\square$  and open triangles  $\triangle$  are from the predictions [Eqs. (49), (50)], while  $\blacklozenge$  and  $\bullet$  are from numerical simulations. Network size is  $N = 100$ . (a) ER random networks, and (b) scale free networks.

estimation of  $\rho \in (\rho^{c1}, \rho^{c2})$ . The roles of the drift term in the Fokker-Plank equation have been disclosed explicitly. The variance of  $\rho^c$  is also obtained analytically provided the network structures  $P(k)$  and  $P(k'|k)$  are given. Therefore, the dynamic process on finite structured populations shows more complex regimes when the initial density of one strategy passes the unstable fixed point  $\rho^*$ .

Our results have been verified by various numerical simulations on random and scale free networks. Here we focused on the coordination games. The stochastic modeling of the dynamic process can be generalized to other classes of network games, for instance, snowdrift games, where metastability of fixation probability may appear on scale free networks [43]. Another interesting problem is to study the change from finite to infinite population structures, for instance, when  $N \rightarrow \infty$  as has been done in [21].

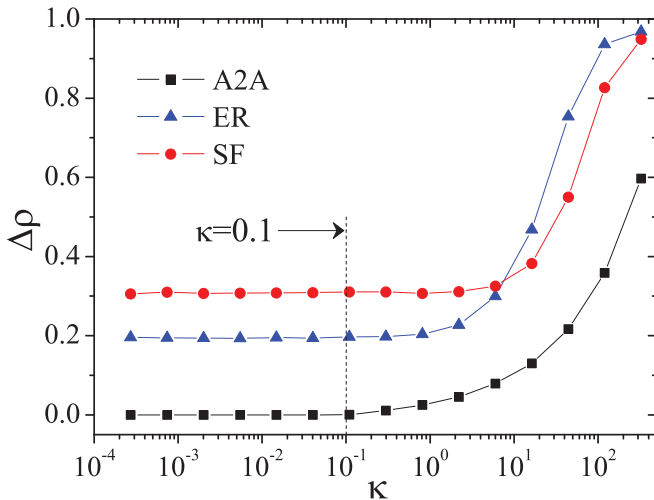


FIG. 7. (Color online) Effects of  $\kappa$  on  $\Delta\rho$  (network size  $N = 100$ ; mean degree  $\langle k \rangle = 10$ ).  $\kappa$  is varied in  $\kappa \in (2.7 \times 10^{-4}, 3.3 \times 10^2)$ , while  $\kappa = 0.1$  is highlighted. ER random networks ( $\blacktriangle$ ), scale free networks ( $\bullet$ ), and well-mixed (all-to-all connected) networks ( $\blacksquare$ ).

In the present work, we concentrated on networked games with two strategies. The situation becomes more challenging when more competitive strategies are coexistent, which yields more complicated dynamic scenarios [44,45]. Furthermore, community structures are often one important characteristic of a complex network. Recently, this idea has been experiencing a fast development, including a proper extension to multiplex or multilayer complex networks [46], with growing structured populations [47,48], or adaptive networks [49]. Evolutionary games on such networks of more complex structures will be a subject for future work. The generalization of our proposed stochastic modeling will be a helpful tool in this line of research.

## ACKNOWLEDGMENTS

This work is in part financially supported by the National Natural Science of China (Grants No. 11305062, No. 11135001, and No. 81471651), the Specialized Research Fund (SRF) for the Doctoral Program (No. 20130076120003), the SRF for ROCS, SEM, the Innovation Program of Shanghai Municipal Education Commission Grant No. 12ZZ043, and the Open Project Program of State Key Laboratory of Theoretical Physics, Institute of Theoretical Physics, Chinese Academy of Sciences, China (No.Y4KF151CJ1).

## APPENDIX: TRANSITION MATRIX $M$

As we have discussed in Sec. III [Eq. (4)], the crucial step is to obtain the state transition matrix  $M$ . The fixation probabilities and the averaged fixation times are calculated by Eqs. (16) and (18). In this section, we provide a general framework in obtaining the fundamental matrix  $H$  of the stochastic process [15].

Let us assume  $v(j)$  to be the number of necessary steps to reach one transient state  $\phi_j$  (neither the final absorbing state  $\phi_0$  nor  $\phi_N$  is arrived). We denote  $\mu_m(j) = 1$  when the system reaches the state  $\phi_j$  after  $m$  steps, and  $\mu_m(j) = 0$  if otherwise. With this notation, we have  $v(j) = \sum_{m=0}^{\infty} \mu_m(j)$ .

Starting from any transient state  $\phi_i$ , the mean time that the system needs to reach the other transient state  $\phi_j$  is expressed as

$$E_i(v(j)) = E_i\left(\sum_{m=0}^{\infty} \mu_m(j)\right) = \sum_{m=0}^{\infty} E_i(\mu_m(j)) = \sum_{m=0}^{\infty} [(1 - M_{ij}^{(m)}) \times 0 + M_{ij}^{(m)} \times 1] = \sum_{m=0}^{\infty} M_{ij}^{(m)}. \quad (\text{A1})$$

For any two transient states  $i, j \in Q$ , we have

$$(E_i(v(j)))_{i,j \in Q} = I + Q + Q^2 + \cdots = (I_{N-1} - Q)^{-1} = H. \quad (\text{A2})$$

With the fundamental matrix  $H$ , one derives the fixation probabilities and expectation times as Eqs. (18) and (19).

- 
- [1] J. M. Smith, *Evolution and the Theory of Games* (Cambridge University Press, Cambridge, England, 1982).
- [2] J. Hofbauer and K. Sigmund, *Evolutionary Games and Population Dynamics* (Cambridge University Press, Cambridge, England, 1998).
- [3] M. A. Nowak and R. M. May, *Nature (London)* **359**, 826 (1992).
- [4] G. Szabó and G. Fáth, *Phys. Rep.* **446**, 97 (2007).
- [5] A. Arenas, A. Díaz-Guilera, J. Kurths, Y. Moreno, and C. S. Zhou, *Phys. Rep.* **469**, 93 (2008).
- [6] E. Lieberman, C. Hauert, and M. A. Nowak, *Nature (London)* **433**, 312 (2005).
- [7] M. A. Nowak, *Science* **314**, 1560 (2006).
- [8] J. Heitzig, K. Lessmann, and Y. Zou, *Proc. Natl. Acad. Sci. USA* **108**, 15739 (2011).
- [9] Y. Zou, T. Pereira, M. Small, Z. Liu, and J. Kurths, *Phys. Rev. Lett.* **112**, 114102 (2014).
- [10] R. Pastor-Satorras and A. Vespignani, *Phys. Rev. Lett.* **86**, 3200 (2001).
- [11] C. P. Roca, J. A. Cuesta, and A. Sanchez, *EPL (Europhys. Lett.)* **87**, 48005 (2009).
- [12] P.-P. Li, J. Ke, Z. Lin, and P. M. Hui, *Phys. Rev. E* **85**, 021111 (2012).
- [13] F. C. Santos, M. D. Santos, and J. M. Pacheco, *Nature (London)* **454**, 213 (2008).
- [14] M. A. Nowak, A. Sasaki, C. Taylor, and D. Fudenberg, *Nature (London)* **428**, 646 (2004).
- [15] N. van Kampen, *Stochastic Processes in Physics and Chemistry*, 3rd ed. (Elsevier, Amsterdam, 2007).
- [16] C. Taylor, D. Fudenberg, A. Sasaki, and M. Nowak, *Bull. Math. Biol.* **66**, 1621 (2004).
- [17] T. Antal and I. Scheuring, *Bull. Math. Biol.* **68**, 1923 (2006).
- [18] D. Zhou and H. Qian, *Phys. Rev. E* **84**, 031907 (2011).
- [19] A. Traulsen and C. Hauert, in *Reviews of Nonlinear Dynamics and Complexity*, edited by H.-G. Schuster (Wiley-VCH Verlag GmbH & Co. KGaA, Berlin, 2009), Vol. 2, pp. 25–61.
- [20] T. Galla, *J. Theor. Biol.* **269**, 46 (2011).
- [21] A. Traulsen, J. C. Claussen, and C. Hauert, *Phys. Rev. Lett.* **95**, 238701 (2005).
- [22] A. Traulsen, M. A. Nowak, and J. M. Pacheco, *Phys. Rev. E* **74**, 011909 (2006).
- [23] M. Mobilia, *Phys. Rev. E* **86**, 011134 (2012).
- [24] M. Assaf and M. Mobilia, *J. Stat. Mech.: Theory Exp.* (2010) P09009.
- [25] M. Assaf, M. Mobilia, and E. Roberts, *Phys. Rev. Lett.* **111**, 238101 (2013).
- [26] A. J. Black, A. Traulsen, and T. Galla, *Phys. Rev. Lett.* **109**, 028101 (2012).
- [27] A. Traulsen, J. C. Claussen, and C. Hauert, *Phys. Rev. E* **85**, 041901 (2012).
- [28] T. Antal, S. Redner, and V. Sood, *Phys. Rev. Lett.* **96**, 188104 (2006).
- [29] K. Hashimoto and K. Aihara, *J. Theor. Biol.* **258**, 637 (2009).
- [30] L.-X. Zhong, D.-F. Zheng, B. Zheng, C. Xu, and P. M. Hui, *EPL (Europhys. Lett.)* **76**, 724 (2006).
- [31] L. Cao, H. Ohtsuki, B. Wang, and K. Aihara, *J. Theor. Biol.* **272**, 8 (2011).
- [32] F. Fu and M. Nowak, *J. Stat. Phys.* **151**, 637 (2013).
- [33] K. H. Z. So, H. Ohtsuki, and T. Kato, *J. Stat. Mech.: Theory Exp.* (2014) P10020.
- [34] G. Szabó and C. Tóke, *Phys. Rev. E* **58**, 69 (1998).
- [35] Z. Rong, H.-X. Yang, and W.-X. Wang, *Phys. Rev. E* **82**, 047101 (2010).
- [36] Z. Wang and M. Perc, *Phys. Rev. E* **82**, 021115 (2010).
- [37] M. El-Mikkawy and A. Karawia, *Appl. Math. Lett.* **19**, 712 (2006).
- [38] A. Traulsen, J. M. Pacheco, and L. A. Imhof, *Phys. Rev. E* **74**, 021905 (2006).
- [39] P. M. Altrock and A. Traulsen, *New J. Phys.* **11**, 013012 (2009).
- [40] B. Wu, P. M. Altrock, L. Wang, and A. Traulsen, *Phys. Rev. E* **82**, 046106 (2010).
- [41] F. Fu, L. Wang, M. A. Nowak, and C. Hauert, *Phys. Rev. E* **79**, 046707 (2009).
- [42] P. M. Altrock and A. Traulsen, *Phys. Rev. E* **80**, 011909 (2009).
- [43] M. Assaf and M. Mobilia, *Phys. Rev. Lett.* **109**, 188701 (2012).
- [44] J. C. Claussen and A. Traulsen, *Phys. Rev. Lett.* **100**, 058104 (2008).
- [45] A. Szolnoki, M. Mobilia, L.-L. Jiang, B. Szczesny, A. M. Rucklidge, and M. Perc, *J. R. Soc. Interface* **11**, 20140735 (2014).
- [46] J. Gómez-Gardeñes, C. Gracia-Lázaro, L. M. Floría, and Y. Moreno, *Phys. Rev. E* **86**, 056113 (2012).
- [47] J. Poncela, J. Gómez-Gardeñes, A. Traulsen, and Y. Moreno, *New J. Phys.* **11**, 083031 (2009).
- [48] A. Melbinger, J. Cremer, and E. Frey, *Phys. Rev. Lett.* **105**, 178101 (2010).
- [49] S. Lee, P. Holme, and Z.-X. Wu, *Phys. Rev. Lett.* **106**, 028702 (2011).